HHS Public Access

Author manuscript

Science. Author manuscript; available in PMC 2021 August 07.

Published in final edited form as:

Science. 2018 March 30; 359(6383): 1520–1523. doi:10.1126/science.aal2022.

Erythrocytic ferroportin reduces intracellular iron accumulation, hemolysis, and malaria risk

De-Liang Zhang[1], **Jian Wu**[2], **Binal N. Shah**[3], **Katja C. Greutélaers**[4], **Manik C. Ghosh**[1], **Hayden Ollivierre**[1], **Xin-zhuan Su**[2], **Philip E. Thuma**[5], **George Bedu-Addo**[6], **Frank P. Mockenhaupt**[4], **Victor R. Gordeuk**[3], **Tracey A. Rouault**[1,*]

[1]Section on Human Iron Metabolism, Eunice Kennedy Shriver National Institute of Child Health and Human Development, National Institutes of Health, Bethesda, MD 20892, USA.

[2]Laboratory of Malaria and Vector Research, National Institute of Allergy and Infectious Diseases, National Institutes of Health, Bethesda, MD 20892, USA.

[3]Sickle Cell Center, University of Illinois at Chicago, Chicago, IL 60612, USA.

[4]Charité–Universitätsmedizin Berlin, Freie Universität Berlin, Humboldt-Universität zu Berlin, and Berlin Institute of Health, Institute of Tropical Medicine and International Health, Berlin 13353, Germany.

[5]Malaria Research Trust, Choma 630166, Zambia.

[6]Komfo Anokye Teaching Hospital, Kwame Nkrumah University of Science and Technology, Kumasi, Ghana.

Abstract

Malaria parasites invade red blood cells (RBCs), consume copious amounts of hemoglobin, and severely disrupt iron regulation in humans. Anemia often accompanies malaria disease; however, iron supplementation therapy inexplicably exacerbates malarial infections. Here we found that the iron exporter ferroportin (FPN) was highly abundant in RBCs, and iron supplementation suppressed its activity. Conditional deletion of the *Fpn* gene in erythroid cells resulted in accumulation of excess intracellular iron, cellular damage, hemolysis, and increased fatality in malaria-infected mice. In humans, a prevalent *FPN* mutation, Q248H (glutamine to histidine at position 248), prevented hepcidin-induced degradation of FPN and protected against severe malaria disease. *FPN* Q248H appears to have been positively selected in African populations in

*Corresponding author: rouault@mail.nih.gov.

Author contributions: D.L.Z. designed the project, performed the experiments, analyzed the data, and wrote the paper; T.A.R. supervised the project and wrote the paper; M.C.G. supervised the mouse colonies and reviewed the paper; H.O. performed the mouse experiments and reviewed the paper; J.W. and X.S. performed and analyzed the mouse malarial study and reviewed the paper; B.N.S., V.R.G., and P.E.T. performed and analyzed the human malaria study for Zambian children and reviewed the paper; K.C.G., G.B.-A., and F.P.M. performed and analyzed the human malaria study for Ghanaian women and reviewed the paper.

Competing interests: All authors declare no competing interests.

Data and materials availability: All data to understand and assess the conclusions of this research are available in the main text and supplementary materials.

SUPPLEMENTARY MATERIALS

www.sciencemag.org/content/359/6383/1520/suppl/DC1

response to the impact of malaria disease. Thus, FPN protects RBCs against oxidative stress and malaria infection.

Humans have coevolved with malaria parasites of the genus *Plasmodium* for millennia (1). Plasmodia invade red blood cells (RBCs) and feed on hemoglobin, and thus, malaria infection profoundly disrupts iron homeostasis, as erythroblasts consume 90% of the daily available iron to produce RBCs. Paradoxically, malaria parasites cannot acquire iron from intact heme (2–5), leaving iron released by hemoglobin autoxidation as the most likely iron source for plasmodia (6–8). Furthermore, for unknown reasons, iron supplementation exacerbates the severity of malarial infections (3, 9–11). However, mechanistic understanding of iron homeostasis in RBCs is surprisingly incomplete because most iron homeostasis proteins are absent in mature RBCs (12, 13).

Ferroportin (FPN) is the only known iron exporter in mammalian cells; it transports iron from enterocytes, hepatocytes, and splenic macrophages into the blood to optimize systemic iron homeostasis (14, 15). FPN expression is regulated in nucleated cells at the translational level by iron regulatory proteins and also posttranslationally by hepcidin, a systemic iron regulatory hormone, to optimize plasma iron homeostasis (16, 17). Recently, we found that FPN was highly expressed in erythroblasts (18, 19). Thus, we hypothesized that FPN is probably present in mature RBCs to export iron generated by hemoglobin autoxidation and thereby protect against iron accumulation, as well as malaria infection.

Confirming our hypothesis, immunoblots with different FPN antibodies detected a strong signal in both mouse and human RBCs, indicating that FPN was present in mature RBCs (Fig. 1A). Next, we deleted the *Fpn* gene specifically in erythroblasts (fig. S1, A to D) (14, 20), which reduced FPN to a faint signal in RBCs of *Fpn* knockout (KO) ($Fpn^{fl/fl};ErCre^{+/-}$) mice (Fig. 1B). In purified cells, the intensity of the FPN signal from RBCs was about 40% of that from erythroblasts, whereas other iron-regulatory proteins, including transferrin receptor 1, divalent metal transporter 1, and iron regulatory protein 1, were not detected in RBCs (Fig. 1C and fig. S2). We further evaluated FPN abundance in a mass-spectrum database of human RBC membranes, which included healthy controls and Diamond-Blackfan anemia (DBA) patients (Table 1 and table S1) (21), and estimated that FPN occurred at 54,000 copies per cell, an amount greater than that of the integral RBC membrane protein component glycophorin C. These results indicated that FPN was highly abundant in mature RBCs.

To evaluate whether FPN on RBC membranes was a functional iron exporter, we loaded RBCs with the radioisotope ^{55}Fe and measured its efflux to the medium (Fig. 1D). Within 60 min, wild-type (WT) RBCs exported 43% of ^{55}Fe to the medium compared with 18% exported by *Fpn* KO RBCs, indicating that erythrocytic FPN exported iron. Surprisingly, exogenous hepcidin reduced ^{55}Fe export from 43 to 30% (Fig. 1D), indicating that hepcidin inhibited FPN activity in mature RBCs. In animals fed on a high-iron diet, FPN levels decreased in RBCs, as hepcidin expression increased (Fig. 1E, fig. S3A). Exogenous hepcidin treatment decreased FPN levels in erythroblasts (Fig. 1F), in which the degradation apparatus is intact, but not in RBCs (Fig. 1G), which lack the proteasomal degradation pathway for hepcidin. Together with findings in DBA patients (22) (Table 1 and table S1)

and sickle cell disease patients (23) (fig. S3, B and C), we observed that RBC FPN levels inversely correlated with hepcidin expression, likely owing to the regulation of FPN in erythroblasts (Fig. 1F). Hepcidin inhibited FPN iron-export activity (Fig. 1D) but did not change FPN abundance on RBCs (Fig. 1G), indicating that hepcidin binding sterically suppressed the iron-export activity of FPN (24, 25).

Fpn knockout increased non-heme iron content and intracellular ferritin levels of erythroblasts (fig. S1, E and F) and resulted in a mild compensated anemia and extramedullary erythropoiesis (figs. S4 to S6 and table S2). The anemia was not caused by a defect of erythroblast differentiation (fig. S7) but instead by the increased fragility and hemolysis of the mature RBCs, as evidenced by the 2.5-fold increase of free plasma hemoglobin after storage at 4°C for 20 hours (Fig. 2, A and B, and fig. S8A). Consistently, we found that the labile iron pool of *Fpn* KO RBCs increased by 80% (Fig. 2C), and non-heme iron and ferritin levels (Fig. 2D and fig. S8B) also significantly increased. Iron overload increased reactive oxygen species production by 30% (Fig. 2, E and F), which damaged RBC plasma membranes, as shown by increased annexin V staining (fig. S8C) and osmotic fragility (Fig. 2G). Consequently, the RBC half-life was reduced from 25 days in WT mice to 14 days in *Fpn* KO mice (Fig. 2H). The shorter life span was attributable to a cell-autonomous defect of *Fpn* KO RBCs, because only 80% of *Fpn* KO RBCs remained in the circulation relative to WT RBCs when their survival was compared in the same animal (Fig. 2I and fig. S9) and the few remaining WT RBCs in the conditional KO mice increased in proportion during the RBC aging process (Fig. 2J and fig. S10). Consistently, serum haptoglobin depletion (Fig. 2K and fig. S11A), increased CD163 and heme oxygenase 1 expression (figs. S11, B and C, and S5F), and iron overload observed in splenic macrophages, Kupffer cells, and renal proximal tubules (fig. S11D) indicated that *Fpn* KO mice were suffering from hemolytic anemia. These results showed that FPN was critical for exporting free iron to maintain the integrity of mature RBCs.

The high abundance of FPN on RBCs, its effects on RBC iron status, and its down-regulation by iron supplementation could therefore influence the growth of malaria parasites (3–5, 9, 10, 26). To test this hypothesis, we intravenously injected WT and *Fpn* KO mice with *Plasmodiumyoelii YM*, a lethal murine malaria strain. *Fpn* KO mice had 60% more parasite-infected RBCs than WT mice on multiple successive days after infection (Fig. 3A), and they died more rapidly after infection (Fig. 3B). We next infected multiple mice with *P. chabaudi chabaudi AS*, a murine strain that almost exclusively infects mature RBCs (fig. S12). Consistently, the parasitemia of *Fpn* KO mice was higher than that of WT mice from days 3 to 6, before reticulocyte numbers increased and mature RBCs declined (Fig. 3C and fig. S12).

Because malaria has long driven the evolution of the human genome (1), we hypothesized that mutations that increased FPN levels would protect humans from malaria infection and be evolutionarily enriched in malaria-endemic regions. The *FPN* Q248H (glutamine to histidine at position 248) mutation occurs in sub-Saharan African populations with a heterozygote prevalence of 2.2 to 20%, depending on location (27–29). The mutation renders FPN resistant to hepcidin-induced degradation (30), and carriers have lower hemoglobin concentrations than controls (29), consistent with our hypothesis that high FPN

levels in erythroblasts export iron and diminish hemoglobin production (18, 19). After screening 27 African Americans, we found three Q248H heterozygotes. Immunoblot analyses confirmed that FPN levels were increased in the RBCs of Q248H heterozygotes relative to control donors (fig. S13), indicating that the mutation could have as yet unknown health consequences in carriers of African descent.

We then analyzed the parasitemia of 66 hospitalized Zambian children with uncomplicated *P. falciparum* malaria who were <6 years of age (Table 2 and table S3) (31, 32). The Q248H mutation was observed in 19.7% of the children (12 heterozygotes, 1 homozygote). Compared to patients with a WT allele, who had a median of 189,667 parasites/μl, Q248H patients had 28,000 parasites/μl (two-sided Fisher's test and chi-square test, $P = 0.025$). Q248H patients also experienced less fulminant malaria, as manifested by tolerance of longer fever times before presentation to the hospital (median of 69 versus 37 hours, Q248H versus WT, $P = 0.1$). Additionally, the hemoglobin concentrations of Q248H patients were lower than those of patients with a WT allele (median of 8.8 versus 10.1 g/dl, Q248H versus WT, $P = 0.1$), which was consistent with the possibility that increased FPN abundance in Q248H carriers reduced the amount of iron available for hemoglobin synthesis (29, 30).

We next investigated the effects of the Q248H mutation on malarial infection in 290 primiparous Ghanaian women (Table 3 and table S4). Primiparae are particularly prone to placental malaria, because acquired immunity against parasites adhering to the placental syncytiotrophoblast is insufficiently developed in the first pregnancy (33). Of 290 women, 8.6% were Q248H carriers (24 heterozygotes, 1 homozygote). Present or past placental *P. falciparum* infection occurred less frequently in Q248H carriers (44.0%) than in women with the respective WT allele (70.2%, $P = 0.007$), even after adjusting by logistic regression for known predictors of placental malaria (34). The apparent protection that the Q248H mutation conferred against malaria infection was also seen in the analysis of peripheral blood samples (44.0 versus 60.4%, $P = 0.11$), even though analysis of peripheral blood is relatively insensitive for diagnosing malaria in pregnant women.

We found that the iron exporter FPN was highly abundant on mature RBCs. FPN prevents erythrocytic iron accumulation and concomitant oxidative stress and protects RBCs against malarial infection (fig. S14). FPN on mature RBCs was abundant under conditions of iron deficiency but diminished with iron supplementation. Its activity was inhibited by hepcidin, which would increase the labile iron pool within RBCs and promote the growth of plasmodial parasites. These findings help to explain why iron deficiency protects against malarial infection, why iron supplementation promotes malaria-related hospitalization and mortality, and why the Q248H mutation may have undergone positive selection in African populations of malaria-endemic regions, among other protective mutations (9, 10, 35).

Supplementary Material

Refer to Web version on PubMed Central for supplementary material.

ACKNOWLEDGMENTS

We thank N. Andrews for providing us the Fpn-flox mice, S. Orkin for providing us the ErCre mice, the Department of Transfusion Medicine of the NIH Clinical Center for providing Buffy Coats for the research, J. Tisdale for providing sickle cell disease samples, and J. Langhorne from The Francis Crick Institute, U.K., for providing *P. chabaudi*.

Funding: This work was supported by the intramural program of the Eunice Kennedy Shriver National Institute of Child Health and Human Development and by the Division of Intramural Research at the National Institute of Allergy and Infectious Diseases (NIAID), NIH.

REFERENCES AND NOTES

1. Cowman AF, Healer J, Marapana D, Marsh K, Cell 167, 610–624 (2016). [PubMed: 27768886]
2. Sigala PA, Crowley JR, Hsieh S, Henderson JP, Goldberg DE, J. Biol. Chem 287, 37793–37807 (2012). [PubMed: 22992734]
3. Clark MA, Goheen MM, Cerami C, Front. Pharmacol 5, 84 (2014). [PubMed: 24834053]
4. Scholl PF, Tripathi AK, Sullivan DJ, Curr. Top. Microbiol. Immunol 295, 293–324 (2005). [PubMed: 16265896]
5. Prentice AM, J. Nutr 138, 2537–2541 (2008). [PubMed: 19022986]
6. Rifkind JM, Nagababu E, Ramasamy S, Ravi LB, Redox Rep. 8, 234–237 (2003). [PubMed: 14962355]
7. Umbreit J, Am. J. Hematol 82, 134–144 (2007). [PubMed: 16986127]
8. Kanias T, Acker JP, FEBS J. 277, 343–356 (2010). [PubMed: 19968714]
9. Sazawal S. et al., Lancet 367, 133–143 (2006). [PubMed: 16413877]
10. Gwamaka M. et al., Clin. Infect. Dis 54, 1137–1144 (2012). [PubMed: 22354919]
11. Spottiswoode N, Duffy PE, Drakesmith H, Front. Pharmacol 5, 125 (2014). [PubMed: 24910614]
12. Zhang DL, Ghosh MC, Rouault TA, Front. Pharmacol 5, 124 (2014). [PubMed: 24982634]
13. Wilkinson N, Pantopoulos K, Front. Pharmacol 5, 176 (2014). [PubMed: 25120486]
14. Donovan A. et al., Cell Metab. 1, 191–200 (2005). [PubMed: 16054062]
15. Drakesmith H, Nemeth E, Ganz T, Cell Metab. 22, 777–787 (2015). [PubMed: 26437604]
16. Abboud S, Haile DJ, J. Biol. Chem 275, 19906–19912 (2000). [PubMed: 10747949]
17. Nemeth E. et al., Science 306, 2090–2093 (2004). [PubMed: 15514116]
18. Zhang DL, Hughes RM, Ollivierre-Wilson H, Ghosh MC,Rouault TA, Cell Metab. 9, 461–473 (2009). [PubMed: 19416716]
19. Zhang DL et al., Blood 118, 2868–2877 (2011). [PubMed: 21700773]
20. Heinrich AC, Pelanda R, Klingmüller U, Blood 104, 659–666 (2004). [PubMed: 15090451]
21. Pesciotta EN et al., PLOS ONE 9, e85504 (2014).
22. Pospisilova D. et al., Haematologica 99, e118–e121 (2014). [PubMed: 24727814]
23. Jenkins ZA et al., Pediatr. Hematol. Oncol 24, 237–243 (2007). [PubMed: 17613866]
24. Taniguchi R. et al., Nat. Commun 6, 8545 (2015). [PubMed: 26461048]
25. Aschemeyer S. et al., Blood 131, 899–910 (2018). [PubMed: 29237594]
26. Schümann K, Solomons NW, Food Nutr. Bull 34, 349–356 (2013). [PubMed: 24167915]
27. Kasvosve I. et al., Am. J. Clin. Nutr 82, 1102–1106 (2005). [PubMed: 16280445]
28. Albuquerque D. et al., Ann. Hum. Biol 38, 378–381 (2011). [PubMed: 21231898]
29. Gordeuk VR et al., Blood Cells Mol. Dis 31, 299–304 (2003). [PubMed: 14636642]
30. Nekhai S. et al., Haematologica 98, 455–463 (2013). [PubMed: 23065513]
31. Molyneux ME, Taylor TE, Wirima JJ, Borgstein A, Q. J. Med 71, 441–459 (1989). [PubMed: 2690177]
32. Thuma PE et al., J. Infect. Dis 203, 211–219 (2011). [PubMed: 21288821]
33. Fried M, Nosten F, Brockman A, Brabin BJ, Duffy PE, Nature 395, 851–852 (1998). [PubMed: 9804416]

34. Grundy MA, Gorman N, Sinclair PR, Chorney MJ, Gerhard GS, J. Biochem. Biophys. Methods 59, 195–200 (2004). [PubMed: 15163531]

35. Murray MJ, Murray AB, Murray MB, Murray CJ, BMJ 2, 1113–1115 (1978). [PubMed: 361162]

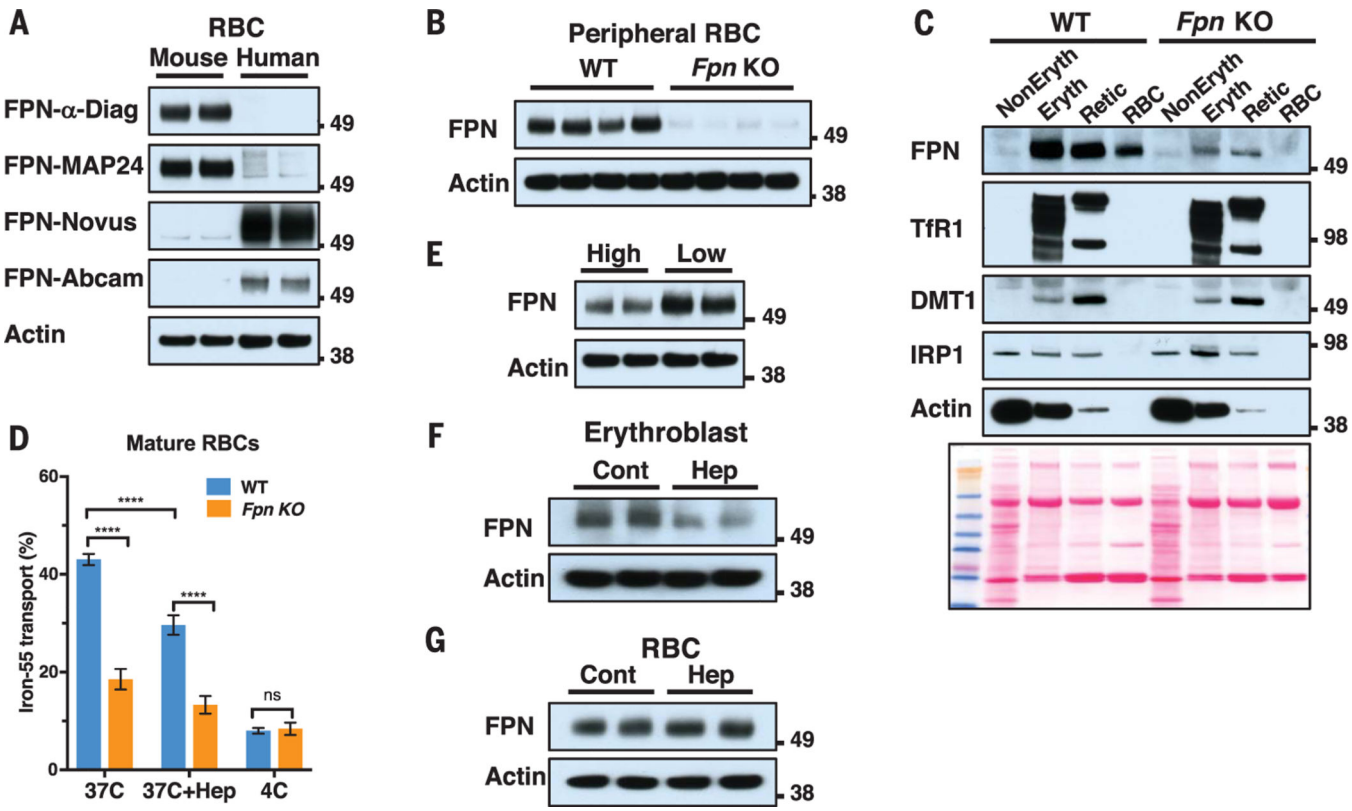

Fig. 1. FPN is highly abundant on mature RBCs, and its activity is inhibited by iron supplementation and hepcidin.

(A) Immunoblots with four different FPN antibodies showed that FPN protein was present in membrane fractions of human and mouse RBCs. Actin is present as a loading control. **(B)** FPN protein levels were reduced in RBCs of erythroblast-specific *Fpn* KO mice. **(C)** FPN was about half as abundant in RBCs as in erythroblasts, but other iron metabolism proteins, including transferrin receptor 1 (TfR1), divalent metal transporter 1 (DMT1), and iron regulatory protein 1 (IRP1), were absent in RBCs (total lysate). Cells were purified by flow cytometry from bone marrow (fig. S2). Bottom image shows Ponceau S staining as a loading control. NonEryth, nonerythroblasts; Eryth, erythroblasts; Retic, reticulocytes. **(D)** Export of Fe^{55} by WT and *Fpn* KO RBCs was measured after 1 hour at 37°C, at 37°C with 1 μg/ml hepcidin (hep), or at 4°C. Mean ± 95% confidence interval (CI); $n = 3$. The experiments were independently repeated three times. Significance was determined by two-way analysis of variance (ANOVA) and Sidak's multiple comparisons test. **** $P < 0.0001$; ns, not significant. **(E)** FPN levels were lower in membranes of RBCs from mice treated on high-iron diets (high) versus low-iron diets (low). Each lane represents a sample from one individual mouse. **(F** and **G)** FPN levels in total lysates of (F) erythroblasts and (G) RBCs treated ex vivo without (cont) or with 1 μg/ml hepcidin (hep) for 24 hours. Two independent replicates are shown in adjacent lanes. Numbers to the right of immunoblots are in kDa.

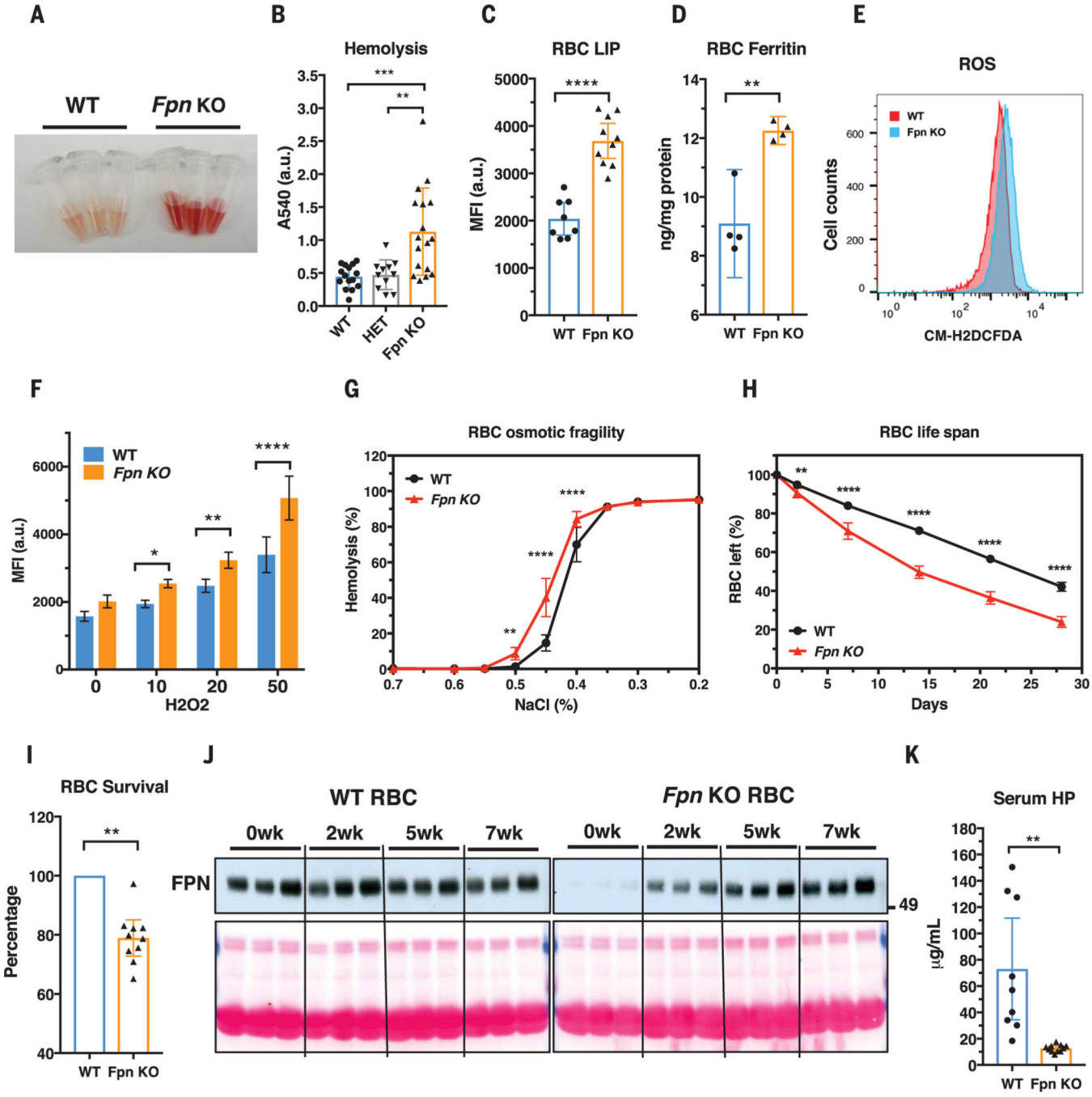

Fig. 2. *Fpn* knockout in erythroblasts leads to RBC iron overload and intravascular hemolysis.

(A) Plasma of WT and *Fpn* KO mice after storing blood samples for 20 hours at 4°C showed increased hemolysis of *Fpn* KO RBCs. **(B)** Free-hemoglobin levels in plasma of WT, heterozygote (HET), and *Fpn* KO mice. Significance determined by one-way ANOVA and Tukey's multiple comparisons test. A540, absorption at 540 nm; a.u., arbitrary units. **(C)** Labile iron pool (LIP) and **(D)** ferritin levels were dramatically increased in RBCs of *Fpn* KO mice. MFI, median fluorescence intensity. **(E)** Representative flow cytometry of reactive oxygen species (ROS) in RBCs of WT and *Fpn* KO mice and **(F)** quantification of ROS

levels in RBCs of WT and *Fpn* KO mice after stimulation by H_2O_2 at different micromolar concentrations. $n = 8$. CM-H2DCFCA is a ROS indicator. **(G)** Osmotic fragility of RBCs, $n = 9$. **(H)** RBC life span of *Fpn* KO mice, $n = 9$. **(I)** Survival of ex vivo biotin-labeled WT and *Fpn* KO RBCs in the same WT mice (fig. S9). **(J)** Immunoblots showing FPN levels in the aging process of the RBCs of three WT and three *Fpn* KO mice in vivo. Sulfo-NHS-LC-Biotin was injected intravenously to label all RBCs, and after 0, 2, 5, and 7 weeks (wk), biotinylated RBCs were purified and FPN levels were then measured with immunoblots in total lysates. Ponceau S staining (bottom) is shown as a loading control. The increase of FPN levels in RBCs of *Fpn* conditional KO mice indicated that the few FPN-expressing RBCs survived longer than *Fpn*-null RBCs and were proportionally enriched over time (fig. S10). **(K)** Serum haptoglobin (HP) was depleted in *Fpn* KO mice. Data are presented as mean ± 95% CI. Significances for (F) to (H) were determined by two-way ANOVA and Sidak's multiple comparisons test; significances for (I) and (K) were determined by Welch's t test. $*P < 0.05$; $**P < 0.01$; $***P < 0.001$; $****P < 0.0001$.

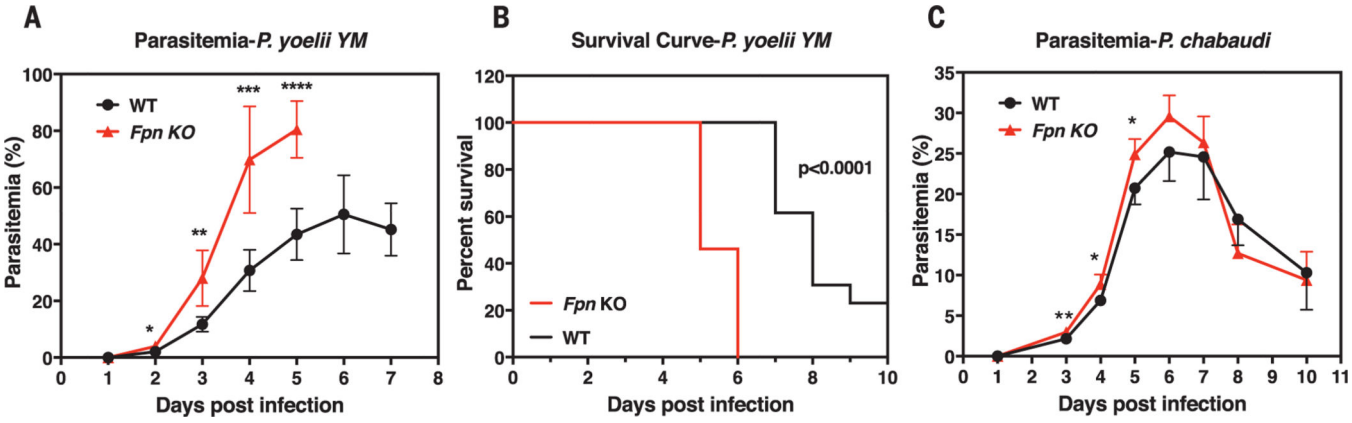

Fig. 3. FPN protects mice from severe malarial infection.

(A) Parasitemia ($n = 5$ for each group) and **(B)** survival curve ($n = 13$ for each group) of WT and *Fpn* KO mice after *P. yoelii YM* infection. **(C)** Parasitemia of WT and *Fpn* KO mice after *P. chabaudi* infection; $n = 5$ for WT and $n = 7$ for *Fpn* KO mice. Data are presented as mean ± 95% CI. Statistical significances determined for (A) and (C) with the Holm-Sidak multiple comparisons test with $\alpha = 0.05$. Survival curves were analyzed with the log-rank test and Gehan-Breslow-Wilcoxon test. *$P < 0.05$; **$P < 0.01$; ***$P < 0.001$; ****$P < 0.0001$.

Table 1.

Mass spectrum analysis shows high abundance of FPN in RBC membrane fractions.

Protein copy number in RBC membrane fractions of control and DBA patients, as reported in mean ± SEM. Data are normalized to Band3, an abundant RBC membrane protein; thus, SEM is not applicable for Band3. Protein 4.1, a major erythrocyte membrane skeleton protein; GLUT1, glucose transporter 1; GYPC, glycophorin C; CYBRD1, cytochrome b reductase 1. See table S3 for details. NA, not applicable.

Protein	Control group (*n* = 4)	DBA group (*n* = 8)	*P* value	Rank*
Band3	1,000,000	1,000,000	NA	5
Prote in 4.1	321,088 ± 8,399	310,758 ± 5,080	0.291	8
GLUT1	153,326 ± 5,628	151,351 ± 2,637	0.720	18
FPN	54,082 ± 1,286	41,694 ± 3,025	0.019	54
GYPC	50,554 ± 2,919	49,348 ± 1,483	0.687	64
CYBRD1	25,158 ± 1977	22,212 ± 1521	0.278	257

*Rank represents the order of the protein on the list when sorted by protein abundance.

Table 2.

***FPN* Q248H mutation was associated with reduced parasitemia in Zambian children with uncomplicated malaria.**

Characteristics of Zambian children with uncomplicated malaria (hematocrit >18% and Blantyre coma score = 5) and either WT or Q248H FPN. Results are presented as median interquartile range. Significances analyzed with Fisher's exact test and chi-square test.

Characteristic	WT (*n* = 53)	Q248H* (*n* = 13)	*P* value
Fever duration before presentation (hours)	37 (21 to 70)	69 (24 to 113)	0.1
Asexual parasites in peripheral blood (parasites/μl)	189,667 (37,108 to 256,129)	28,000 (11,813 to 107,034)	0.025
Hemoglobin (g/dl)	10.1 (8.2 to 11.1)	8.8 (6.6 to 10.3)	0.1

*12 heterozygotes, 1 homozygote.

Table 3.

***FPN* Q248H mutation protected from malarial infection in primiparous Ghanaian women.**

Proportion of *P. falciparum* infection among primiparous Ghanaian women with live singleton delivery and either WTor Q248H FPN. Proportions were compared between groups by chi-square test. PCR, polymerase chain reaction.

Characteristic	All (*n* = 290)	WT (*n* = 265)	Q248H* (*n* = 25)	*P* value
Past or present placental infection†	197/290 (67.9%)	186/265 (70.2%)	11/25 (44%)	0.007
Placental blood *P. falciparum* PCR positivity	188/290 (64.8%)	177/265 (66.8%)	11/25 (44%)	0.03
Peripheral blood *P. falciparum* PCR positivity	171/290 (59%)	160/265 (60.4%)	11/25 (44%)	0.11

*24 heterozygotes, 1 homozygote.

†Microscopic detection of placental parasitemia or malaria pigment, or a positive PCR result on placental blood samples.